

MIT Open Access Articles

Is a color superconductor topological?

The MIT Faculty has made this article openly available. **Please share** how this access benefits you. Your story matters.

Citation: Nishida, Yusuke. "Is a color superconductor topological?." Physical Review D 81.7 (2010): 074004. © 2010 The American Physical Society

As Published: <http://dx.doi.org/10.1103/PhysRevD.81.074004>

Publisher: American Physical Society

Persistent URL: <http://hdl.handle.net/1721.1/58601>

Version: Final published version: final published article, as it appeared in a journal, conference proceedings, or other formally published context

Terms of Use: Article is made available in accordance with the publisher's policy and may be subject to US copyright law. Please refer to the publisher's site for terms of use.



Is a color superconductor topological?

Yusuke Nishida

Center for Theoretical Physics, Massachusetts Institute of Technology, Cambridge, Massachusetts 02139, USA

(Received 18 January 2010; published 5 April 2010)

A fully gapped state of matter, whether insulator or superconductor, can be asked if it is topologically trivial or nontrivial. Here we investigate topological properties of superconducting Dirac fermions in 3D having a color superconductor as an application. In the chiral limit, when the pairing gap is parity even, the right-handed and left-handed sectors of the free space Hamiltonian have nontrivial topological charges with opposite signs. Accordingly, a vortex line in the superconductor supports localized gapless right-handed and left-handed fermions with the dispersion relations $E = \pm v p_z$ (v is a parameter dependent velocity) and thus propagating in opposite directions along the vortex line. However, the presence of the fermion mass immediately opens up a mass gap for such localized fermions and the dispersion relations become $E = \pm v \sqrt{m^2 + p_z^2}$. When the pairing gap is parity odd, the situation is qualitatively different. The right-handed and left-handed sectors of the free space Hamiltonian in the chiral limit have nontrivial topological charges with the same sign and therefore the presence of the small fermion mass does not open up a mass gap for the fermions localized around the vortex line. When the fermion mass is increased further, there is a topological phase transition at $m = \sqrt{\mu^2 + \Delta^2}$ and the localized gapless fermions disappear. We also elucidate the existence of gapless surface fermions localized at a boundary when two phases with different topological charges are connected. A part of our results is relevant to the color superconductivity of quarks.

DOI: [10.1103/PhysRevD.81.074004](https://doi.org/10.1103/PhysRevD.81.074004)

PACS numbers: 21.65.Qr, 12.38.-t

I. INTRODUCTION

A fully gapped state of matter can be asked if it is topologically trivial or nontrivial. The most well-known topological state of matter is the quantum Hall effect in two dimensions (2D) [1–3], in which the time reversal symmetry is explicitly broken. Recently the time reversal symmetric extensions of the quantum Hall effect have been theoretically proposed and experimentally observed both in 2D [4–7] and 3D [8–15], which are referred to as topological insulators (the 2D topological insulator is also known as the quantum spin Hall effect). Generally the topological state of matter is characterized by the nontrivial topological charge of the single-particle Hamiltonian and accompanied by topologically protected gapless edge/surface states with linear dispersions (Dirac fermions).

Another class of topological states of matter arises in superconductors. Although the ordinary nonrelativistic s -wave superconductor is topologically trivial, the weakly paired phase of the $p_x + ip_y$ superconductor in 2D is topologically nontrivial [16] and Sr_2RuO_4 is its candidate material [17]. In addition to the gapless edge/surface states, the vortex in the topological superconductor supports gapless fermions localized around the vortex core. It is also known from the pioneering work by Jackiw and Rossi that the relativistic s -wave superconductor in 2D has the similar properties [18]. Such a system has recently received renewed interest because it can be realized on the surface of the 3D topological insulator in contact with the s -wave

superconductor [19]. It is pointed out that the Balian-Werthamer state realized in the B phase of the superfluid ^3He is also topological [20–23].

Such progress on the discoveries of the topological insulators and superconductors motivates us to ask the following question: Is a color superconductor topological? In order to shed light on this question, we investigate in this paper the topological properties of superconducting Dirac fermions in 3D. In Sec. II, we start with the mean-field model Hamiltonian of the color superconductivity of quarks and point it out that the free space Hamiltonian can be characterized by a \mathbb{Z} valued topological charge. In Sec. III, we compute the topological charge of the free space Hamiltonian when the pairing gap is parity even as a function of the fermion mass and show that its value is closely linked to the existence of gapless fermions localized around a vortex line. The low-energy spectrum of such fermions is also determined in this section.

In Sec. IV, we turn to the case where the pairing gap is parity odd. By studying the topological charge of the free space Hamiltonian, we show that there is a topological phase transition as a function of the fermion mass, which is also reflected in the existence of gapless fermions localized around a vortex line. In Sec. V, we elucidate the existence of gapless surface fermions localized at a boundary when two phases with different topological charges are connected. Finally, Sec. VI is devoted to the summary of this paper and implications of our results for the color superconductor are discussed.

II. PREPARATIONS

A. Model Hamiltonian for the color superconductor

We start with the following mean-field model Hamiltonian for the color superconductivity of quarks [24]:

$$H_{\text{CSC}} = \int dx \left[\psi_{a,f}^\dagger (-i\boldsymbol{\alpha} \cdot \boldsymbol{\partial} + \beta m - \mu) \delta_{ab} \delta_{fg} \psi_{b,g} + \frac{1}{2} \psi_{a,f}^\dagger \Delta_{ab,fg}(\mathbf{x}) C \gamma^5 \psi_{b,g}^* - \frac{1}{2} \psi_{a,f}^T \Delta_{ab,fg}^\dagger(\mathbf{x}) C \gamma^5 \psi_{b,g} \right]. \quad (1)$$

Here $C \equiv i\gamma^2\gamma^0$ is the charge conjugation matrix and we assumed the same mass m and the same chemical potential μ for all three colors (a, b) and all three flavors (f, g). $\Delta_{ab,fg}$ is the pairing gap in the Lorentz singlet and even parity ($J^P = 0^+$) channel and its color and flavor structure is specified by

$$\Delta_{ab,fg}(\mathbf{x}) = \sum_{i=1,2,3} \Delta_i(\mathbf{x}) \epsilon_{iab} \epsilon_{ifg}. \quad (2)$$

$\Delta_1 = \Delta_2 = \Delta_3 \neq 0$ corresponds to the fully gapped color-flavor-locked (CFL) phase and $\Delta_1 = \Delta_2 = 0, \Delta_3 \neq 0$ corresponds to the two flavor pairing phase where only four quarks are gapped. In either case, an appropriate transformation of $\psi_{a,f}$ by a real and orthogonal matrix in the color and flavor space can bring the Hamiltonian (1) into the decoupled form $H_{\text{CSC}} = \sum_{j=1}^9 H_j$, where

$$H_j = \int dx \left[\psi_j^\dagger (-i\boldsymbol{\alpha} \cdot \boldsymbol{\partial} + \beta m - \mu) \psi_j + \frac{1}{2} \psi_j^\dagger \Delta_j(\mathbf{x}) C \gamma^5 \psi_j^* - \frac{1}{2} \psi_j^T \Delta_j^*(\mathbf{x}) C \gamma^5 \psi_j \right] \\ = \frac{1}{2} \int dx \begin{pmatrix} \psi_j^\dagger & -\psi_j^T C \gamma^5 \end{pmatrix} \\ \times \begin{pmatrix} -i\boldsymbol{\alpha} \cdot \boldsymbol{\partial} + \beta m - \mu & \Delta_j(\mathbf{x}) \\ \Delta_j^*(\mathbf{x}) & i\boldsymbol{\alpha} \cdot \boldsymbol{\partial} - \beta m + \mu \end{pmatrix} \\ \times \begin{pmatrix} \psi_j \\ C \gamma^5 \psi_j^* \end{pmatrix} \\ \equiv \frac{1}{2} \int dx \Psi_j^\dagger \mathcal{H}_j \Psi_j. \quad (3)$$

For example, in the CFL phase, we have $\Delta_{1,2,3} = -\Delta_{4,\dots,8} = \frac{1}{2}\Delta_9$. Below we concentrate on one sector with the nonzero gap $\Delta_j \neq 0$ and suppress the index of j .

The single-particle Hamiltonian \mathcal{H} in the Nambu-Gor'kov representation has the charge conjugation symmetry:

$$C^{-1} \mathcal{H} C = -\mathcal{H}^* \quad \text{with} \quad C \equiv \begin{pmatrix} 0 & -C\gamma^5 \\ C\gamma^5 & 0 \end{pmatrix}. \quad (4)$$

Because $\mathcal{H}\Phi = E\Phi$ leads to $\mathcal{H}(C\Phi^*) = -E(C\Phi^*)$, the

spectrum is symmetric under $E \leftrightarrow -E$. Furthermore, when the phase of $\Delta(\mathbf{x})$ is uniform over the space (i.e. no super-current), one can choose $\Delta(\mathbf{x})$ to be a real function.¹ Then \mathcal{H} has the time reversal symmetry:

$$\mathcal{T}^{-1} \mathcal{H} \mathcal{T} = \mathcal{H}^* \quad \text{with} \quad \mathcal{T} \equiv \begin{pmatrix} \gamma^1 \gamma^3 & 0 \\ 0 & \gamma^1 \gamma^3 \end{pmatrix}. \quad (5)$$

Because $\mathcal{H}\Phi = E\Phi$ leads to $\mathcal{H}(\mathcal{T}\Phi^*) = E(\mathcal{T}\Phi^*)$ and $\Phi^\dagger \mathcal{T}\Phi^* = 0$, the spectrum is at least doubly degenerate. Therefore, we find that our Hamiltonian \mathcal{H} belongs to the symmetry class DIII in the terminology of Refs. [25,26].²

In Sec. IV, we will also consider the case where the pairing takes place in the odd parity channel ($J^P = 0^-$). Such a case is described by simply replacing $\Delta(\mathbf{x})$ in Eqs. (1) and (3) with $\gamma^5 \Delta(\mathbf{x})$. The resulting Hamiltonian has the same charge conjugation and time reversal symmetries and thus belongs to the symmetry class DIII again.

B. Topological charge for class DIII Hamiltonians in 3D

According to Ref. [20], fully gapped 3D Hamiltonians belonging to the symmetry class DIII can be classified by a \mathbb{Z} valued topological charge. The topological charge is defined for the free space Hamiltonian where $\Delta(\mathbf{x}) = \Delta^*(\mathbf{x}) = \Delta_0$ is a constant. Suppose the single-particle Hamiltonian in the momentum space $\mathcal{H}_p \equiv e^{-ip \cdot x} \mathcal{H} e^{ip \cdot x}$ is diagonalized as

$$\mathcal{H}_p = U_p \begin{pmatrix} D_p & 0 \\ 0 & -D_p \end{pmatrix} U_p^\dagger, \quad (6)$$

where U_p is a unitary matrix and D_p is a diagonal matrix with positive elements. For the fully gapped Hamiltonian, we can adiabatically deform D_p into the identity matrix, which continuously deforms the Hamiltonian into a ‘‘new Hamiltonian’’ Q_p defined by

$$Q_p \equiv U_p \begin{pmatrix} \mathbb{1} & 0 \\ 0 & -\mathbb{1} \end{pmatrix} U_p^\dagger \quad (7)$$

with properties $Q_p = Q_p^\dagger$ and $Q_p^2 = 1$. Because of the charge conjugation and time reversal symmetries, a unitary transformation can bring the Hermitian matrix Q_p into a block off-diagonal form [27]:

$$Q_p \rightarrow \begin{pmatrix} 0 & q_p \\ q_p^\dagger & 0 \end{pmatrix}. \quad (8)$$

$Q_p^2 = 1$ leads to $q_p q_p^\dagger = 1$ and thus q_p is a unitary matrix [U(4) in our case]. The topological charge is provided by the winding number of q_p associated with the homotopy group $\pi_3[U(n \geq 2)] = \mathbb{Z}$:

¹If we did not make this choice, we need to modify the definition of \mathcal{T} .

²Class DIII Hamiltonians are meant to have the charge conjugation and time reversal symmetries with properties $C^T = C$ and $\mathcal{T}^T = -\mathcal{T}$ [20].

$$N \equiv \frac{1}{24\pi^2} \int d\mathbf{p} \epsilon^{ijk} \text{Tr}[(q_p^{-1} \partial_i q_p)(q_p^{-1} \partial_j q_p)(q_p^{-1} \partial_k q_p)]. \quad (9)$$

When a given Hamiltonian has a nonzero topological charge, such a system is said to be *topological*. Because Hamiltonians having different topological charges can not be continuously deformed into each other without closing energy gaps in their spectrum, the topological charge defined in Eq. (9) classifies 3D Hamiltonians belonging to the symmetry class DIII [20].

It is known in the case of the $p_x + ip_y$ superconductor in 2D that a nontrivial topological charge of the free space Hamiltonian has a close connection to the existence of a localized zero energy state in the presence of a vortex [16,28]. We will see in the subsequent sections that the same correspondence is true in our Hamiltonian (3) describing superconducting Dirac fermions in 3D. We shall work in the chiral representation:

$$\boldsymbol{\alpha} = \gamma^0 \boldsymbol{\gamma} = \begin{pmatrix} \boldsymbol{\sigma} & 0 \\ 0 & -\boldsymbol{\sigma} \end{pmatrix}, \quad \beta = \gamma^0 = \begin{pmatrix} 0 & \mathbb{1} \\ \mathbb{1} & 0 \end{pmatrix}, \quad (10)$$

and

$$\boldsymbol{\gamma}^5 = \begin{pmatrix} \mathbb{1} & 0 \\ 0 & -\mathbb{1} \end{pmatrix}. \quad (11)$$

III. EVEN PARITY PAIRING

We first consider the case where the pairing takes place in the even parity channel, which is relevant to the color superconductivity of quarks [29,30].

A. Topological charge of a free space Hamiltonian

When the pairing gap is a constant, we can choose it to be real; $\Delta(\mathbf{x}) = \Delta^*(\mathbf{x}) = \Delta_0$. From Eq. (3), the free space Hamiltonian in the momentum space is given by

$$\mathcal{H}_p = \begin{pmatrix} \boldsymbol{\alpha} \cdot \mathbf{p} + \beta m - \mu & \Delta_0 \\ \Delta_0 & -\boldsymbol{\alpha} \cdot \mathbf{p} - \beta m + \mu \end{pmatrix}. \quad (12)$$

Its energy eigenvalues have the usual form

$$E_p = \pm \sqrt{(\sqrt{m^2 + \mathbf{p}^2} \pm \mu)^2 + \Delta_0^2} \quad (13)$$

and each of them are doubly degenerate (signs are not correlated). Note that the spectrum is fully gapped as long as $\Delta_0 \neq 0$. The computation of its topological charge is lengthy but straightforward.³ In order to elucidate the

³Note that the topological charge is invariant as long as the spectrum is fully gapped. Therefore one can set $\mu \rightarrow 0$ to reduce the computational complication.

effect of the fermion mass, we shall present the results for the $m = 0$ case and the $m \neq 0$ case separately.

1. Chiral limit $m = 0$

In the chiral limit $m = 0$, because the right-handed sector and the left-handed sector of the Hamiltonian (12) are decoupled, the unitary matrix q_p in Eq. (8) has the block diagonal form:

$$q_p = \begin{pmatrix} q_{Rp} & 0 \\ 0 & q_{Lp} \end{pmatrix}. \quad (14)$$

Accordingly, we can define the topological charges for the right-handed sector and for the left-handed sector independently. The results are⁴

$$\begin{aligned} N_R &\equiv \frac{1}{24\pi^2} \int d\mathbf{p} \epsilon^{ijk} \text{Tr}[(q_{Rp}^{-1} \partial_i q_{Rp})(q_{Rp}^{-1} \partial_j q_{Rp}) \\ &\quad \times (q_{Rp}^{-1} \partial_k q_{Rp})] \\ &= \frac{\Delta_0}{2|\Delta_0|} \end{aligned} \quad (15)$$

and

$$\begin{aligned} N_L &\equiv \frac{1}{24\pi^2} \int d\mathbf{p} \epsilon^{ijk} \text{Tr}[(q_{Lp}^{-1} \partial_i q_{Lp})(q_{Lp}^{-1} \partial_j q_{Lp}) \\ &\quad \times (q_{Lp}^{-1} \partial_k q_{Lp})] \\ &= -\frac{\Delta_0}{2|\Delta_0|}. \end{aligned} \quad (16)$$

We find that each sector is topologically nontrivial having the nonzero topological charge.⁵ This implies the existence of a localized zero energy state for each sector in the presence of a vortex. However, their signs are opposite and the total topological charge of the Hamiltonian (12) is vanishing; $N = N_R + N_L = 0$.

2. Nonzero fermion mass $m \neq 0$

When the fermion mass is nonzero $m \neq 0$, the right-handed and left-handed sectors are coupled and thus the only total topological charge N is well defined. Because the spectrum is fully gapped for $\Delta_0 \neq 0$, the inclusion of the fermion mass can not change the topological charge. Therefore we find

$$N = 0 \quad (17)$$

for arbitrary m , which means that the system is topologically trivial. In the following subsection, we will see how these observations in the free space are reflected in the spectrum of fermions localized around a vortex line.

⁴The topological charge for the full Hamiltonian (1) can be obtained by simply summing contributions from all gapped sectors.

⁵The half-integer value of N is common to relativistic fermions because q_p is noncompact at $|\mathbf{p}| \rightarrow \infty$. See, e.g., Ref. [20].

B. Spectrum of fermions localized around a vortex line

The spectrum of fermions in the presence of a singly quantized vortex line is obtained by solving the Bogoliubov–de Gennes equation:

$$\begin{pmatrix} -i\boldsymbol{\alpha} \cdot \boldsymbol{\partial} + \beta m - \mu & e^{i\theta} |\Delta(r)| \\ e^{-i\theta} |\Delta(r)| & i\boldsymbol{\alpha} \cdot \boldsymbol{\partial} - \beta m + \mu \end{pmatrix} \Phi(\mathbf{x}) = E\Phi(\mathbf{x}). \quad (18)$$

Here we assumed that the vortex line extends in the z direction and $\Delta(\mathbf{x})$ does not depend on z ; $\Delta(\mathbf{x}) = e^{i\theta} |\Delta(r)|$ where (r, θ, z) are cylindrical polar coordinates. Note that we do not make any assumptions on the form of $|\Delta(r)|$ except that it has a nonvanishing asymptotic value; $|\Delta(r \rightarrow \infty)| > 0$. Therefore the existence of localized fermions that we will find below is independent of the vortex profile and thus in this sense they are *universal*. This would be because these solutions have topological origins and, in particular, the zero energy solutions are guaranteed by the index theorem [18,31]. In contrast, there will be other Caroli–de Gennes–Matricon-type bound fermions on the vortex line which typically have the energy gap $\sim |\Delta(\infty)|^2/\mu$ [32]. Because their spectrum depends on the vortex profile, we shall not investigate such nonuniversal solutions in this paper.

Because of the translational invariance in the z direction, we look for solutions of the form

$$\Phi(r, \theta, z) = e^{ip_z z} \phi_{p_z}(r, \theta). \quad (19)$$

We rewrite the Hamiltonian in Eq. (18) as

$$\begin{aligned} e^{-ip_z z} \mathcal{H} e^{ip_z z} &= \mathcal{H}|_{m=p_z=0} \\ &+ \begin{pmatrix} \alpha_z p_z + \beta m & 0 \\ 0 & -\alpha_z p_z - \beta m \end{pmatrix} \\ &\equiv \mathcal{H}_0 + \delta \mathcal{H}. \end{aligned} \quad (20)$$

We first construct zero energy solutions for \mathcal{H}_0 at $m = p_z = 0$ and then determine their dispersion relations with treating $\delta \mathcal{H}$ ($m, p_z \neq 0$) as a perturbation.

1. Zero energy solutions at $m = p_z = 0$

Consider the zero energy Bogoliubov–de Gennes equation at $m = p_z = 0$; $\mathcal{H}_0 \phi_0 = 0$. We can find two exponentially localized solutions (see Appendix A):

$$\phi_R \equiv \frac{e^{i(\pi/4)}}{\sqrt{\lambda}} \begin{pmatrix} J_0(\mu r) \\ ie^{i\theta} J_1(\mu r) \\ 0 \\ 0 \\ e^{-i\theta} J_1(\mu r) \\ -iJ_0(\mu r) \\ 0 \\ 0 \end{pmatrix} e^{-\int_0^r |\Delta(r')| dr'} \quad (21)$$

and

$$\phi_L \equiv \frac{e^{-i(\pi/4)}}{\sqrt{\lambda}} \begin{pmatrix} 0 \\ 0 \\ J_0(\mu r) \\ -ie^{i\theta} J_1(\mu r) \\ 0 \\ 0 \\ e^{-i\theta} J_1(\mu r) \\ iJ_0(\mu r) \end{pmatrix} e^{-\int_0^r |\Delta(r')| dr'}, \quad (22)$$

where λ is a normalization constant:

$$\lambda = 2\pi \int_0^\infty dr r [2J_0^2(\mu r) + 2J_1^2(\mu r)] e^{-2\int_0^r |\Delta(r')| dr'}. \quad (23)$$

These two solutions have definite chirality; $\gamma^5 \phi_{R/L} = \pm \phi_{R/L}$, and hence their index.

2. Perturbations in terms of m and p_z

We now evaluate matrix elements of $\delta \mathcal{H}$ with respect to ϕ_R and ϕ_L . It is easy to find

$$\begin{aligned} &\int_0^{2\pi} d\theta \int_0^\infty dr r \begin{pmatrix} \phi_R^\dagger \delta \mathcal{H} \phi_R & \phi_R^\dagger \delta \mathcal{H} \phi_L \\ \phi_L^\dagger \delta \mathcal{H} \phi_R & \phi_L^\dagger \delta \mathcal{H} \phi_L \end{pmatrix} \\ &= v \begin{pmatrix} p_z & -im \\ im & -p_z \end{pmatrix}, \end{aligned} \quad (24)$$

where we defined the parameter dependent velocity $|v| \leq 1$ in units of the speed of light:

$$v \equiv \frac{\int_0^\infty dr r [J_0^2(\mu r) - J_1^2(\mu r)] e^{-2\int_0^r |\Delta(r')| dr'}}{\int_0^\infty dr r [J_0^2(\mu r) + J_1^2(\mu r)] e^{-2\int_0^r |\Delta(r')| dr'}}. \quad (25)$$

Therefore, when $m = 0$, the right-handed and left-handed fermions localized around the vortex line have the gapless dispersion relations:

$$E = vp_z \quad \text{and} \quad E = -vp_z, \quad (26)$$

respectively. They have opposite velocities and thus propagate in opposite directions along the vortex line (Fig. 1). In the simple case where $|\Delta(r)| = \Delta > 0$ is a constant, the velocity v in Eq. (25) can be evaluated as

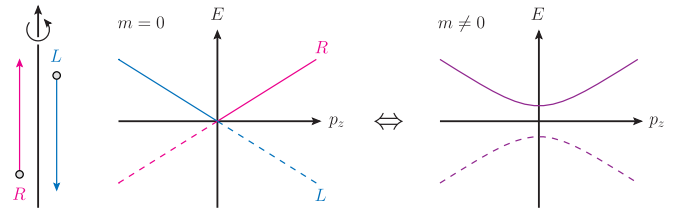


FIG. 1 (color online). Low-energy spectrum of fermions localized around the vortex line in the chiral limit (left panel) and with the nonzero fermion mass for the even parity pairing (right panel). The $E < 0$ part of the spectrum is redundant in the superconductor and thus shown by the dashed line.

$$v = \frac{\mu^2}{\mu^2 + \Delta^2} \frac{\mathcal{E}(-\mu^2/\Delta^2)}{\mathcal{E}(-\mu^2/\Delta^2) - \mathcal{K}(-\mu^2/\Delta^2)} - 1$$

$$\rightarrow \begin{cases} (\ln \frac{4\mu}{\Delta} - 1) (\frac{\Delta}{\mu})^2 + \dots & (\frac{\Delta}{\mu} \rightarrow 0) \\ 1 - \frac{3}{4} (\frac{\mu}{\Delta})^2 + \dots & (\frac{\Delta}{\mu} \rightarrow \infty) \end{cases}, \quad (27)$$

which is plotted in Fig. 2 as a function of Δ/μ . Here $\mathcal{K}(\mathcal{E})$ is the complete elliptic integral of the first (second) kind.

On the other hand, when $m \neq 0$, the right-handed and left-handed fermions are mixed and their spectrum exhibits the mass gap provided by vm (Fig. 1):

$$E = \pm v \sqrt{m^2 + p_z^2}. \quad (28)$$

This is closely linked to our previous observations on the topological charge of the free space Hamiltonian. In the chiral limit $m = 0$, each of the right-handed and left-handed sectors is topologically nontrivial ($N_R = -N_L \neq 0$) and thus the vortex line supports the localized gapless fermions. However, once the fermion mass $m \neq 0$ is introduced, the total Hamiltonian is topologically trivial ($N = 0$) and thus the vortex line no longer supports the gapless fermions. Nevertheless, as long as $vm \ll \Delta$ ($r \rightarrow \infty$) is satisfied, the mass gap of such localized fermions is much smaller than the energy gap of bulk fermions and thus they can be important low-energy degrees of freedom.

3. Nonperturbative solutions at $\mu = 0$

The above results rely on the perturbations in terms of m and p_z . In the special case where $\mu = 0$, we can obtain the exact dispersion relations of the localized fermions and their eigenfunctions with arbitrary m and p_z (see Appendix A). The two solutions to the Bogoliubov–de Gennes equation (18) at $\mu = 0$ are found to be

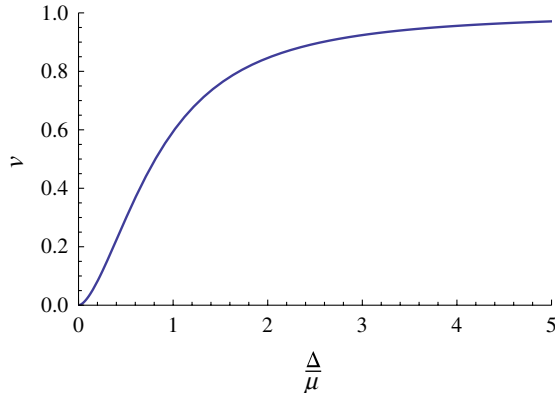


FIG. 2 (color online). The velocity v in Eq. (27) as a function of Δ/μ .

$$\Phi_{\pm}(r, \theta, z) = \frac{e^{-i(\pi/4)}}{\sqrt{\lambda_{\pm}}} \begin{pmatrix} p_z + E_{\pm} \\ 0 \\ m \\ 0 \\ 0 \\ -i(p_z + E_{\pm}) \\ 0 \\ im \end{pmatrix} e^{ip_z z - \int_0^r |\Delta(r')| dr'} \quad (29)$$

with $E_{\pm} = \pm \sqrt{m^2 + p_z^2}$. The discussions given above are valid in this special case too.

C. Effective 1D Hamiltonian along a vortex line

Because the bulk fermions are gapped, the low-energy effective Hamiltonian of the system in the chiral limit $m = 0$ should involve the gapless fermions existing along the vortex line. In order to write down the effective 1D Hamiltonian, we expand the fermion operator Ψ in Eq. (3) in terms of the eigenfunctions of \mathcal{H} :

$$\Psi(\mathbf{x}) = \int \frac{dp_z}{2\pi} (a_{p_z} e^{ip_z z} \phi_R + b_{p_z} e^{ip_z z} \phi_L + \dots), \quad (30)$$

where a_{p_z} and b_{p_z} are quasiparticle operators associated with the gapless right-handed and left-handed fermions, respectively. Because of the pseudoreality condition $\Psi = \mathcal{C}\Psi^*$ and the property of the solutions $\mathcal{C}\phi_{R/L}^* = \phi_{R/L}$, we have $a_{p_z}^{\dagger} = a_{-p_z}$ and $b_{p_z}^{\dagger} = b_{-p_z}$. The quasiparticle operators obeying such conditions are called as *Majorana fermions* in condensed matter literatures [16,19–22]. From the Hamiltonian $H = \frac{1}{2} \int dx \Psi^{\dagger} \mathcal{H} \Psi$, the effective 1D Hamiltonian becomes

$$H_{1D} = \frac{v}{2} \int \frac{dp_z}{2\pi} (p_z a_{p_z}^{\dagger} a_{p_z} - p_z b_{p_z}^{\dagger} b_{p_z}). \quad (31)$$

When the nonzero fermion mass $m \neq 0$ is present, there are additional terms mixing a_{p_z} and b_{p_z} :

$$H_{1D} = \frac{v}{2} \int \frac{dp_z}{2\pi} (p_z a_{p_z}^{\dagger} a_{p_z} - p_z b_{p_z}^{\dagger} b_{p_z} + im b_{p_z}^{\dagger} a_{p_z} - im a_{p_z}^{\dagger} b_{p_z}). \quad (32)$$

IV. ODD PARITY PAIRING

So far we have discussed the case where the pairing takes place in the even parity channel. The situation is qualitatively different when the pairing takes place in the odd parity channel [$\Delta(\mathbf{x}) \rightarrow \gamma^5 \Delta(\mathbf{x})$].

A. Topological charge of a free space Hamiltonian

When the pairing gap is a constant $\Delta(\mathbf{x}) = \Delta^*(\mathbf{x}) = \Delta_0$, the free space Hamiltonian in the momentum space is given by

$$\mathcal{H}_p = \begin{pmatrix} \boldsymbol{\alpha} \cdot \mathbf{p} + \beta m - \mu & \gamma^5 \Delta_0 \\ \gamma^5 \Delta_0 & -\boldsymbol{\alpha} \cdot \mathbf{p} - \beta m + \mu \end{pmatrix}. \quad (33)$$

Its energy eigenvalues have the form

$$E_p = \pm \sqrt{m^2 + \mathbf{p}^2 + \mu^2 + \Delta_0^2 \pm 2\sqrt{m^2(\mu^2 + \Delta_0^2) + \mathbf{p}^2 \mu^2}} \quad (34)$$

and each of them are doubly degenerate (signs are not correlated). Note that even if $\Delta_0 \neq 0$, the energy gap in the spectrum is closed at $m^2 = \mu^2 + \Delta_0^2$. This fact will have important consequences on the topological charge of the free space Hamiltonian and thus on the existence of localized zero energy states in the presence of a vortex.

1. Chiral limit $m = 0$

In the chiral limit $m = 0$, we can define the topological charges for the right-handed sector and for the left-handed sector independently. Compared to the even parity pairing, γ^5 in front of Δ_0 flips the sign of the pairing gap only in the left-handed sector. Therefore, from Eqs. (15) and (16), we easily obtain

$$N_R = \frac{\Delta_0}{2|\Delta_0|} \quad \text{and} \quad N_L = \frac{\Delta_0}{2|\Delta_0|}. \quad (35)$$

We find that each sector is topologically nontrivial having the nonzero topological charge. The striking difference of the odd parity pairing from the even parity pairing is that their signs are the same and thus the total topological charge of the Hamiltonian (33) is nonvanishing;

$$N = N_R + N_L = \frac{\Delta_0}{|\Delta_0|}. \quad (36)$$

This implies, unlike the even parity pairing, that the existence of localized zero energy states in the presence of a vortex is robust against the inclusion of the small fermion mass.

2. Nonzero fermion mass $m \neq 0$

When the fermion mass is nonzero $m \neq 0$, the only total topological charge N is well defined. Because the spectrum remains gapped as long as $m^2 < \mu^2 + \Delta_0^2$, the topological charge remains the same; $N = \Delta_0/|\Delta_0|$. However, when the fermion mass exceeds the critical value $m^2 = \mu^2 + \Delta_0^2$ at which the energy gap in the spectrum closes, there is a quantum phase transition to another fully gapped phase characterized by its vanishing topological charge⁶:

⁶This phase is continuously connected to the Hamiltonian with $\mu, \Delta_0 \rightarrow 0$ where the topological charge can be computed most easily.

$$N = \begin{cases} \frac{\Delta_0}{|\Delta_0|} & \text{for } m^2 < \mu^2 + \Delta_0^2 \\ 0 & \text{for } m^2 > \mu^2 + \Delta_0^2. \end{cases} \quad (37)$$

Because these two phases can not be distinguished by symmetries, the phase transition between them is a *topological phase transition*. This is exactly the same type of the topological phase transition occurring in the 2D $p_x + ip_y$ superconductor at $\mu = 0$ as a function of the chemical potential [16,28]. Other quantum phase transitions resulting from the momentum space topology are extensively discussed in Ref. [33]. In the following subsection, we will see how these observations in the free space are reflected in the existence of gapless fermions localized around a vortex line.

B. Spectrum of fermions localized around a vortex line

The spectrum of fermions in the presence of a singly quantized vortex line is obtained by solving the Bogoliubov–de Gennes equation:

$$\begin{pmatrix} -i\boldsymbol{\alpha} \cdot \boldsymbol{\partial} + \beta m - \mu & \gamma^5 e^{i\theta} |\Delta(r)| \\ \gamma^5 e^{-i\theta} |\Delta(r)| & i\boldsymbol{\alpha} \cdot \boldsymbol{\partial} - \beta m + \mu \end{pmatrix} \Phi(\mathbf{x}) = E\Phi(\mathbf{x}). \quad (38)$$

As we stated in Sec. III B, we do not make any assumptions on the form of $|\Delta(r)|$ except that it has a nonvanishing asymptotic value; $|\Delta(r \rightarrow \infty)| > 0$. Because of the translational invariance in the z direction, we look for solutions of the form

$$\Phi(r, \theta, z) = e^{ip_z z} \phi_{p_z}(r, \theta). \quad (39)$$

We rewrite the Hamiltonian in Eq. (38) as

$$\begin{aligned} e^{-ip_z z} \mathcal{H} e^{ip_z z} &= \mathcal{H}|_{p_z=0} + \begin{pmatrix} \alpha_z p_z & 0 \\ 0 & -\alpha_z p_z \end{pmatrix} \\ &\equiv \mathcal{H}_0 + \delta\mathcal{H}. \end{aligned} \quad (40)$$

We first construct zero energy solutions for \mathcal{H}_0 at $p_z = 0$ and then determine their dispersion relations with treating $\delta\mathcal{H}$ ($p_z \neq 0$) as a perturbation.

1. Zero energy solutions at $p_z = 0$

Consider the zero energy Bogoliubov–de Gennes equation at $p_z = 0$; $\mathcal{H}_0 \phi_0 = 0$. We can find two potentially normalizable solutions (see Appendix B):

$$\phi_R \equiv \frac{e^{i(\pi/4)}}{\sqrt{\lambda}} \begin{pmatrix} \mu \bar{J}_0 \\ i\sqrt{\mu^2 - m^2} e^{i\theta} \bar{J}_1 \\ m \bar{J}_0 \\ 0 \\ \sqrt{\mu^2 - m^2} e^{-i\theta} \bar{J}_1 \\ -i\mu \bar{J}_0 \\ 0 \\ -im \bar{J}_0 \end{pmatrix} e^{-\int_0^r |\Delta(r')| dr'} \quad (41)$$

and

$$\phi_L \equiv \frac{e^{i(\pi/4)}}{\sqrt{\lambda}} \begin{pmatrix} m\bar{J}_0 \\ 0 \\ \mu\bar{J}_0 \\ -i\sqrt{\mu^2 - m^2}e^{i\theta}\bar{J}_1 \\ 0 \\ -im\bar{J}_0 \\ -\sqrt{\mu^2 - m^2}e^{-i\theta}\bar{J}_1 \\ -i\mu\bar{J}_0 \end{pmatrix} e^{-\int_0^r |\Delta(r')| dr'}, \quad (42)$$

where we introduced shorthand notations; $\bar{J}_0 \equiv J_0(\sqrt{\mu^2 - m^2}r)$ and $\bar{J}_1 \equiv J_1(\sqrt{\mu^2 - m^2}r)$, and λ is a normalization constant:

$$\lambda = 2\pi \int_0^\infty dr r [2(\mu^2 + m^2)\bar{J}_0^2 + 2(\mu^2 - m^2)\bar{J}_1^2] e^{-2\int_0^r |\Delta(r')| dr'}. \quad (43)$$

These two solutions in the chiral limit $m = 0$ have definite chirality; $\gamma^5 \phi_{R/L} = \pm \phi_{R/L}$, and hence their index. Note that, although the nonzero fermion mass $m \neq 0$ mixes the right-handed and left-handed fermions, their gaplessness is preserved.

We now examine if the above two solutions are normalizable or not. When $m^2 < \mu^2$, they are normalizable owing to the exponentially decaying factor $e^{-\int_0^r |\Delta(r')| dr'} \rightarrow e^{-r|\Delta(\infty)|}$ at $r \rightarrow \infty$. When $m^2 > \mu^2$, we note that $\bar{J}_0 = I_0(\sqrt{m^2 - \mu^2}r)$ and $\bar{J}_1 = iI_1(\sqrt{m^2 - \mu^2}r)$ exponentially grow as $\bar{J}_0, \bar{J}_1 \rightarrow e^{\sqrt{m^2 - \mu^2}r}$. Nevertheless, as long as $m^2 < \mu^2 + |\Delta(\infty)|^2$ is satisfied, the exponentially decaying factor dominates and the solutions are still normalizable. However, when the fermion mass exceeds the critical value $m^2 = \mu^2 + |\Delta(\infty)|^2$, the two solutions exponentially grow and thus they are no longer acceptable solutions. Therefore we find that the gapless fermions localized around the vortex line exist only when $m^2 < \mu^2 + |\Delta(\infty)|^2$ and they disappear when $m^2 > \mu^2 + |\Delta(\infty)|^2$.

Of course this is closely linked to our previous observations on the topological charge of the free space Hamiltonian; it is topologically nontrivial ($N \neq 0$) for $m^2 < \mu^2 + |\Delta_0|^2$ and trivial ($N = 0$) for $m^2 > \mu^2 + |\Delta_0|^2$ and there is a topological phase transition in between. Also note the striking difference of the odd parity pairing from the even parity pairing where the presence of the fermion mass immediately opened up a mass gap for the fermions localized around the vortex line.

2. Perturbation in terms of p_z

We now evaluate matrix elements of $\delta\mathcal{H}$ with respect to ϕ_R and ϕ_L for $m^2 < \mu^2 + |\Delta(\infty)|^2$. It is easy to find

$$\begin{aligned} & \int_0^{2\pi} d\theta \int_0^\infty dr r \begin{pmatrix} \phi_R^\dagger \delta\mathcal{H} \phi_R & \phi_R^\dagger \delta\mathcal{H} \phi_L \\ \phi_L^\dagger \delta\mathcal{H} \phi_R & \phi_L^\dagger \delta\mathcal{H} \phi_L \end{pmatrix} \\ & = v \begin{pmatrix} p_z & 0 \\ 0 & -p_z \end{pmatrix}, \end{aligned} \quad (44)$$

where we defined the parameter dependent velocity $|v| \leq 1$ in units of the speed of light:

$$v \equiv \frac{\int_0^\infty dr r [(\mu^2 - m^2)\bar{J}_0^2 - (\mu^2 - m^2)\bar{J}_1^2] e^{-2\int_0^r |\Delta(r')| dr'}}{\int_0^\infty dr r [(\mu^2 + m^2)\bar{J}_0^2 + (\mu^2 - m^2)\bar{J}_1^2] e^{-2\int_0^r |\Delta(r')| dr'}}. \quad (45)$$

Therefore the dispersion relations of the gapless fermions localized around the vortex line are given by

$$E = vp_z \quad \text{and} \quad E = -vp_z. \quad (46)$$

They have opposite velocities and thus propagate in opposite directions along the vortex line. In the simple case where $|\Delta(r)| = \Delta > 0$ is a constant, the velocity v in Eq. (45) can be evaluated as

$$v = \frac{\mu^2 \bar{\mathcal{E}}}{(\mu^2 + \Delta^2)\bar{\mathcal{E}} - (\mu^2 + \Delta^2 - m^2)\bar{\mathcal{K}}} - 1, \quad (47)$$

where $\bar{\mathcal{K}} \equiv \mathcal{K}((m^2 - \mu^2)/\Delta^2)$ and $\bar{\mathcal{E}} \equiv \mathcal{E}((m^2 - \mu^2)/\Delta^2)$. When $m = 0$, this is identical to Eq. (27) and plotted in Fig. 2 as a function of Δ/μ . The velocity vanishes at $m = \mu$ and changes its sign for $m > \mu$.

3. Nonperturbative solutions at $\mu = 0$

The above results rely on the perturbation in terms of p_z . In the special case where $\mu = 0$, we can obtain the exact dispersion relations of the localized fermions and their eigenfunctions with arbitrary p_z (see Appendix B). The two solutions to the Bogoliubov–de Gennes equation (38) at $\mu = 0$ are found to be

$$\Phi(r, \theta, z) = \frac{e^{i(\pi/4)}}{\sqrt{\lambda'}} \begin{pmatrix} I_0(mr) \\ 0 \\ 0 \\ ie^{i\theta}I_1(mr) \\ 0 \\ -iI_0(mr) \\ e^{-i\theta}I_1(mr) \\ 0 \end{pmatrix} e^{ip_z z - \int_0^r |\Delta(r')| dr'} \quad (48)$$

with $E = p_z$ and

$$\Phi(r, \theta, z) = \frac{e^{i(\pi/4)}}{\sqrt{\lambda'}} \begin{pmatrix} 0 \\ -ie^{i\theta}I_1(mr) \\ I_0(mr) \\ 0 \\ -e^{-i\theta}I_1(mr) \\ 0 \\ 0 \\ -iI_0(mr) \end{pmatrix} e^{ip_z z - \int_0^r |\Delta(r')| dr'} \quad (49)$$

with $E = -p_z$. They are normalizable in the x - y plane as long as $m < \Delta(\infty)$. The discussions given above are valid in this special case too.

C. Effective 1D Hamiltonian along a vortex line

Because the bulk fermions are gapped, the low-energy effective Hamiltonian of the system with $m^2 < \mu^2 + |\Delta(\infty)|^2$ should involve the gapless fermions existing along the vortex line. In order to write down the effective 1D Hamiltonian, we expand the fermion operator Ψ in Eq. (3) in terms of the eigenfunctions of \mathcal{H} :

$$\Psi(\mathbf{x}) = \int \frac{dp_z}{2\pi} (a_{p_z} e^{ip_z z} \phi_R + b_{p_z} e^{ip_z z} \phi_L + \dots), \quad (50)$$

where a_{p_z} and b_{p_z} are Majorana quasiparticle operators obeying $a_{p_z}^\dagger = a_{-p_z}$ and $b_{p_z}^\dagger = b_{-p_z}$ and associated with the two gapless fermions. From the Hamiltonian $H = \frac{1}{2} \times \int dx \Psi^\dagger \mathcal{H} \Psi$, the effective 1D Hamiltonian becomes

$$H_{1D} = \frac{v}{2} \int \frac{dp_z}{2\pi} (p_z a_{p_z}^\dagger a_{p_z} - p_z b_{p_z}^\dagger b_{p_z}). \quad (51)$$

V. BOUNDARY PROBLEMS

In Secs. III and IV, we have discussed the connection between the nonzero topological charge of the free space Hamiltonian and the existence of localized gapless fermions in the presence of a vortex. Another characteristic of the topological state of matter is the existence of gapless edge/surface states when it is terminated by another gapped state having a different topological charge. In this section, we will investigate two types of boundary problems and elucidate the existence of gapless surface fermions localized at the boundary.

A. Boundary between $\Delta_0 > 0$ and $\Delta_0 < 0$

We first consider the boundary where the pairing gap $\Delta(\mathbf{x}) = \Delta(z)$ changes its sign as ($\Delta_\infty > 0$):

$$\Delta(z) \rightarrow \begin{cases} +\Delta_\infty & \text{for } z \rightarrow \infty \\ -\Delta_\infty & \text{for } z \rightarrow -\infty. \end{cases} \quad (52)$$

Because the topological charge of the free space Hamiltonian, when it is nonzero, depends on the sign of the pairing gap [see Eqs. (15), (16), and (35)], the above boundary connects two gapped phases with different topological charges and thus we expect the gapless fermions localized at the boundary. Here we present the low-energy spectrum of such fermions and their effective 2D Hamiltonian. Their derivations are analogous to those in the vortex problems and some details are provided in Appendix C.

1. Chiral limit $m = 0$

In the chiral limit $m = 0$, we can find gapless right-handed and left-handed fermions localized at the boundary. Their dispersion relations are given by

$$E = \pm |v| \sqrt{p_x^2 + p_y^2}, \quad (53)$$

where $\mathbf{p}_\perp \equiv (p_x, p_y)$ is the momentum parallel to the boundary and $|v| \leq 1$ is the parameter dependent velocity in units of the speed of light:

$$v = \frac{\int_{-\infty}^{\infty} dz e^{2i\mu z - 2 \int_0^z \Delta(z') dz'}}{\int_{-\infty}^{\infty} dz e^{-2 \int_0^z \Delta(z') dz'}}. \quad (54)$$

In the simple case with $\Delta(z) = \Delta_\infty \text{sgn}(z)$, the velocity can be evaluated as $v = \Delta_\infty^2 / (\Delta_\infty^2 + \mu^2)$. The low-energy effective Hamiltonian involving the two gapless fermions existing at the 2D boundary becomes

$$H_{2D} = \frac{|v|}{2} \int \frac{d\mathbf{p}_\perp}{(2\pi)^2} [a_{\mathbf{p}_\perp}^\dagger (\boldsymbol{\sigma}_\perp \cdot \mathbf{p}_\perp) a_{\mathbf{p}_\perp} - b_{\mathbf{p}_\perp}^\dagger (\boldsymbol{\sigma}_\perp \cdot \mathbf{p}_\perp) b_{\mathbf{p}_\perp}] \quad (55)$$

with $\boldsymbol{\sigma}_\perp \equiv (\sigma_1, \sigma_2)$. Here $a_{\mathbf{p}_\perp}$ and $b_{\mathbf{p}_\perp}$ are two-component Majorana quasiparticle operators obeying $a_{\mathbf{p}_\perp}^\dagger = a_{-\mathbf{p}_\perp}^T \sigma_1$ and $b_{\mathbf{p}_\perp}^\dagger = b_{-\mathbf{p}_\perp}^T \sigma_1$.

2. Even parity pairing with $m \neq 0$

As we can expect from the topological charge of the free space Hamiltonian [Eqs. (17) and (37)], the effect of the nonzero fermion mass $m \neq 0$ is qualitatively different for the even parity pairing and the odd parity pairing. When the pairing gap is parity even, the presence of the fermion mass immediately opens up a mass gap for the fermions localized at the boundary and the dispersion relations become

$$E = \pm |v| \sqrt{m^2 + p_x^2 + p_y^2}. \quad (56)$$

This is linked to the fact that the two phases at both sides $z \rightarrow \pm\infty$ have the same topological charge $N = 0$. Now the effective 2D Hamiltonian has additional terms mixing $a_{\mathbf{p}_\perp}$ and $b_{\mathbf{p}_\perp}$:

$$H_{2D} = \frac{|v|}{2} \int \frac{d\mathbf{p}_\perp}{(2\pi)^2} [a_{\mathbf{p}_\perp}^\dagger (\boldsymbol{\sigma}_\perp \cdot \mathbf{p}_\perp) a_{\mathbf{p}_\perp} - b_{\mathbf{p}_\perp}^\dagger (\boldsymbol{\sigma}_\perp \cdot \mathbf{p}_\perp) b_{\mathbf{p}_\perp} + im b_{\mathbf{p}_\perp}^\dagger a_{\mathbf{p}_\perp} - ima_{\mathbf{p}_\perp}^\dagger b_{\mathbf{p}_\perp}]. \quad (57)$$

3. Odd parity pairing with $m \neq 0$

On the other hand, when the pairing gap is parity odd, the two phases at both sides have different topological charges $N = \pm 1$ even in the presence of the small fermion mass. Accordingly, the boundary still supports the two localized gapless fermions [Eqs. (53) and (55)] with the modified velocity $|v| \leq 1$:

$$v = \frac{\sqrt{\mu^2 - m^2}}{\mu} \frac{\int_{-\infty}^{\infty} dz e^{2i\sqrt{\mu^2 - m^2}z - 2 \int_0^z \Delta(z') dz'}}{\int_{-\infty}^{\infty} dz e^{-2 \int_0^z \Delta(z') dz'}} \quad (58)$$

for $m^2 < \mu^2$ and

$$v = \frac{\sqrt{m^2 - \mu^2}}{m} \quad (59)$$

for $\mu^2 < m^2 < \mu^2 + \Delta_{\infty}^2$.

When the fermion mass is increased further and exceeds the critical value $m^2 = \mu^2 + \Delta_{\infty}^2$, the resulting solutions are no longer normalizable [see Eqs. (C3) and (C9)] and the gapless surface fermions disappear. This is linked to the fact that the two phases at both sides $z \rightarrow \pm\infty$ have the same topological charge $N = 0$ as a consequence of the topological phase transition.

B. Boundary between superconductor and vacuum

We then consider the following boundary that models the interface between the superconductor at $z < 0$ and the chiral symmetry broken vacuum at $z > 0$:

$$\begin{aligned} \mu, \Delta > 0, \quad m = 0 \quad \text{for } z < 0 \\ \mu = \Delta = 0, \quad m > 0 \quad \text{for } z > 0. \end{aligned} \quad (60)$$

For the even parity pairing, the two gapped phases at both sides have the same topological charge $N = 0$, while they have different topological charges for the odd parity pairing; $N = 1$ at $z < 0$ and $N = 0$ at $z > 0$.

Accordingly, when the pairing gap is parity odd, we can find one gapless fermion localized at the boundary $z = 0$. The corresponding two zero energy solutions at $p_x = p_y = 0$ are given by

$$\Phi(\mathbf{x}) \propto \begin{pmatrix} e^{i\mu z} \\ 0 \\ -ie^{-i\mu z} \\ 0 \\ ie^{i\mu z} \\ 0 \\ e^{-i\mu z} \\ 0 \end{pmatrix} e^{\Delta z}, \quad \begin{pmatrix} 0 \\ e^{-i\mu z} \\ 0 \\ ie^{i\mu z} \\ 0 \\ -ie^{i\mu z} \\ 0 \\ e^{i\mu z} \end{pmatrix} e^{\Delta z} \quad (61)$$

for $z < 0$ and

$$\Phi(\mathbf{x}) \propto \begin{pmatrix} 1 \\ 0 \\ -i \\ 0 \\ i \\ 0 \\ 1 \\ 1 \end{pmatrix} e^{-mz}, \quad \begin{pmatrix} 0 \\ 1 \\ 0 \\ i \\ 0 \\ -i \\ 0 \\ 1 \end{pmatrix} e^{-mz} \quad (62)$$

for $z > 0$. Its effective 2D Hamiltonian becomes

$$H_{2D} = \frac{|v|}{2} \int \frac{d\mathbf{p}_{\perp}}{(2\pi)^2} [a_{\mathbf{p}_{\perp}}^{\dagger} (\boldsymbol{\sigma}_{\perp} \cdot \mathbf{p}_{\perp}) a_{\mathbf{p}_{\perp}}] \quad (63)$$

with the velocity $v = (1 + \frac{m}{\Delta + i\mu}) / (1 + \frac{m}{\Delta})$ and the Majorana condition $a_{\mathbf{p}_{\perp}}^{\dagger} = a_{-\mathbf{p}_{\perp}}^T \sigma_1$. However, when the pairing gap is parity even, we cannot find such localized zero energy solutions that are continuous at the boundary $z = 0$ and therefore gapless surface fermions do not exist.

VI. SUMMARY AND CONCLUDING REMARKS

Motivated by the recent discoveries of the topological insulators and superconductors, we have investigated the topological properties of superconducting Dirac fermions in 3D both for the even parity pairing and the odd parity pairing. The results are summarized in Table I. In the chiral limit $m = 0$, we find that the system is topologically non-trivial in the sense that each of the right-handed and left-handed sectors of the free space Hamiltonian has the non-zero topological charge; $N_{R,L} \neq 0$. Accordingly, a vortex line in the superconductor supports localized gapless right-handed and left-handed fermions. Their dispersion relations are given by $E = \pm v p_z$, where $|v| \leq 1$ defined in Eq. (25) is the parameter dependent velocity, and thus they propagate in opposite directions along the vortex line.

The effect of the nonzero fermion mass $m \neq 0$ is qualitatively different for the even parity pairing and the odd parity pairing. When the pairing gap is parity even, the presence of the fermion mass immediately opens up a mass gap for the fermions localized around the vortex line and the dispersion relations become $E = \pm v \sqrt{m^2 + p_z^2}$. This can be understood from the vanishing total topological charge of the free space Hamiltonian for the even parity pairing; $N(= N_R + N_L) = 0$.

On the other hand, when the pairing gap is parity odd, the total topological charge of the free space Hamiltonian is nonvanishing $N \neq 0$ and thus the system remains topological even in the presence of the small fermion mass. Accordingly, the vortex line still supports the localized gapless fermions. When the fermion mass is increased further, there is a topological phase transition at $m = \sqrt{\mu^2 + \Delta^2}$, where the topological charge jumps from the nonzero value to zero and consequently the gapless fermions localized around the vortex line disappear.

TABLE I. Summary of the topological charge of the free space Hamiltonian and the low-energy spectrum of fermions localized around a vortex line (or a boundary where the pairing gap changes its sign). v is a parameter dependent velocity.

	even parity pairing		odd parity pairing	
	topological charge	mid-gap state dispersion	topological charge	mid-gap state dispersion
$m = 0$	$N_R = -N_L = \frac{\Delta_0}{2 \Delta_0 }$	$E = \pm v p_z$	$N_R = N_L = \frac{\Delta_0}{2 \Delta_0 }$	$E = \pm v p_z$
$m \neq 0$	$N = 0$	$E = \pm v \sqrt{m^2 + p_z^2}$	$N = \frac{\Delta_0}{ \Delta_0 }$ $N = 0$	$E = \pm v p_z$ ($m^2 < \mu^2 + \Delta_0^2$) none ($m^2 > \mu^2 + \Delta_0^2$)

Our results for the even parity pairing are relevant to the color superconductivity of quarks. In the CFL phase where all nine quarks are gapped, the mean-field model Hamiltonian for the color superconductor (1) has the topological charge $N_R = -N_L = \sum_{j=1}^9 \frac{\Delta_j}{2|\Delta_j|}$ in the chiral limit $m = 0$. Therefore the $U(1)_B$ vortex line that arises when the CFL quark matter is rotated [34,35] supports nine sets of localized gapless right-handed and left-handed quarks. In the presence of the small quark mass or chiral condensate, such localized quarks become gapped but their mass gap vm is much smaller than the energy gap of bulk quarks Δ .⁷ Furthermore, the mass gap at high density $vm \sim m(\Delta/\mu)^2 \ln(\mu/\Delta)$ [see Eq. (27)] is parametrically smaller than the masses of pseudo-Nambu-Goldstone bosons $\sim m(\Delta/\mu)$ in the CFL phase [36], which are important to the transport properties and neutrino emissivity of the CFL quark matter [24]. Whether such new low-energy degrees of freedom localized around the vortex line have some impact on the physics of rotating neutron/quark stars is an important problem and should be investigated in a future work.

Our results for the odd parity pairing might be irrelevant to the color superconductivity of quarks. Nevertheless it would be interesting to consider if the topological phase transition found in this paper can be realized in condensed matter systems where the 2D Dirac fermions appear.

Finally, Table I reveals the intriguing connection between the nonzero topological charge of the free space Hamiltonian and the existence of localized gapless fermions in the presence of a vortex. We also elucidated the existence of gapless surface fermions localized at a boundary when two phases with different topological charges are connected. The mathematical proof of these correspondences remains an open question.

ACKNOWLEDGMENTS

The author thanks R. Jackiw and F. Wang for many useful discussions and K. Rajagopal for reading the manuscript. This work was supported by MIT Department of Physics Pappalardo Program.

⁷Supposing $\mu \sim 500$ MeV, $\Delta \sim 50$ MeV, and $m \sim 10$ MeV and using Eq. (36), we can estimate the mass gap to be as small as $vm/\Delta \sim 5 \times 10^{-3}$.

Note added.—After the submission of this paper, there appeared a paper by S. Yasui, K. Itakura, and M. Nitta [37] which has some overlap with the present paper. In their paper, a non-Abelian vortex in the CFL phase is also considered.

APPENDIX A: DERIVATIONS OF SOLUTIONS FOR EVEN PARITY PAIRING

Here we outline how the solutions to the Bogoliubov-de Gennes equation (18) for the even parity pairing are derived. We introduce notations

$$\Phi(r, \theta, z) = \begin{pmatrix} F_R \\ F_L \\ G_R \\ G_L \end{pmatrix} e^{ip_z z}, \quad (\text{A1})$$

where $F_{R(L)}$ and $G_{R(L)}$ are right-handed (left-handed) two-component fields. We first make an ansatz

$$F_R(r, \theta) = \begin{pmatrix} f_{R\uparrow}(r) \\ e^{i\theta} f_{R\downarrow}(r) \end{pmatrix} e^{-\int_0^r |\Delta(r')| dr'} \quad (\text{A2})$$

and

$$G_R(r, \theta) = \begin{pmatrix} e^{-i\theta} g_{R\uparrow}(r) \\ g_{R\downarrow}(r) \end{pmatrix} e^{-\int_0^r |\Delta(r')| dr'} \quad (\text{A3})$$

and the same for $R \rightarrow L$ so that they are exponentially localized in the x - y plane. Then we look for $f_{R(L)}$ and $g_{R(L)}$ that are regular at origin and independent of $|\Delta(r)|$. $|\Delta(r)|$ can be eliminated from the equations by imposing

$$g_R = -i\sigma_1 f_R \quad \text{and} \quad g_L = i\sigma_1 f_L. \quad (\text{A4})$$

Now f_R and f_L satisfy the following four sets of equations:

$$\begin{pmatrix} -\mu & \frac{1}{i}(\partial_r + \frac{1}{r}) \\ \frac{1}{i}\partial_r & -\mu \end{pmatrix} f_R = 0 \quad (\text{A5a})$$

$$\begin{pmatrix} p_z - E & 0 \\ 0 & -p_z - E \end{pmatrix} f_R + m f_L = 0 \quad (\text{A5b})$$

$$\begin{pmatrix} \mu & \frac{1}{i}(\partial_r + \frac{1}{r}) \\ \frac{1}{i}\partial_r & \mu \end{pmatrix} f_L = 0 \quad (\text{A5c})$$

$$\begin{pmatrix} -p_z - E & 0 \\ 0 & p_z - E \end{pmatrix} f_L + m f_R = 0. \quad (\text{A5d})$$

We can find consistent solutions in two cases; $m = p_z = E = 0$ [Eqs. (21) and (22)] and $\mu = 0$ [Eq. (29)].

APPENDIX B: DERIVATIONS OF SOLUTIONS FOR ODD PARITY PAIRING

Here we outline how the solutions to the Bogoliubov–de Gennes equation (38) for the odd parity pairing are derived. We use the same notations as in Appendix A. In this case, $|\Delta(r)|$ can be eliminated from the equations by imposing

$$g_R = -i\sigma_1 f_R \quad \text{and} \quad g_L = -i\sigma_1 f_L. \quad (\text{B1})$$

Now f_R and f_L satisfy the following four sets of equations:

$$\begin{pmatrix} -\mu & \frac{1}{i}(\partial_r + \frac{1}{r}) \\ \frac{1}{i}\partial_r & -\mu \end{pmatrix} f_R + m f_L = 0 \quad (\text{B2a})$$

$$\begin{pmatrix} p_z - E & 0 \\ 0 & -p_z - E \end{pmatrix} f_R = 0 \quad (\text{B2b})$$

$$\begin{pmatrix} \mu & \frac{1}{i}(\partial_r + \frac{1}{r}) \\ \frac{1}{i}\partial_r & \mu \end{pmatrix} f_L - m f_R = 0 \quad (\text{B2c})$$

$$\begin{pmatrix} -p_z - E & 0 \\ 0 & p_z - E \end{pmatrix} f_L = 0. \quad (\text{B2d})$$

We can find consistent solutions in two cases; $p_z = E = 0$ [Eqs. (41) and (42)] and $\mu = 0$ [Eqs. (48) and (49)].

APPENDIX C: DERIVATIONS OF SOLUTIONS FOR BOUNDARY PROBLEMS

Here we outline how the spectrum of fermions in the presence of the boundary (52) studied in Sec. VA is obtained. The Bogoliubov–de Gennes equation to be solved is

$$\begin{pmatrix} -i\boldsymbol{\alpha} \cdot \boldsymbol{\partial} + \beta m - \mu & (\gamma_5)\Delta(z) \\ (\gamma_5)\Delta(z) & i\boldsymbol{\alpha} \cdot \boldsymbol{\partial} - \beta m + \mu \end{pmatrix} \Phi(\mathbf{x}) = E\Phi(\mathbf{x}). \quad (\text{C1})$$

Because of the translational invariance in the x - y plane, we look for solutions of the form

$$\Phi(\mathbf{x}) = e^{ip_x x + ip_y y} \phi_{p_x, p_y}(z). \quad (\text{C2})$$

We first make an ansatz

$$\phi_{p_x, p_y}(z) = \begin{pmatrix} f_R(z) \\ f_L(z) \\ g_R(z) \\ g_L(z) \end{pmatrix} e^{-\int_0^z \Delta(z') dz'} \quad (\text{C3})$$

so that the solution is exponentially localized in the z direction. Then we look for $f_{R(L)}$ and $g_{R(L)}$ that are independent of $\Delta(z)$. $\Delta(z)$ can be eliminated from the equations by imposing

$$g_R = -i\sigma_3 f_R \quad \text{and} \quad g_L = \pm i\sigma_3 f_L, \quad (\text{C4})$$

where the upper (lower) sign corresponds to the even (odd) parity pairing. Now f_R and f_L satisfy the following four sets of equations:

$$\begin{pmatrix} \frac{\partial_z}{i} - \mu - E & p_- \\ p_+ & -\frac{\partial_z}{i} - \mu - E \end{pmatrix} f_R + m f_L = 0 \quad (\text{C5a})$$

$$\begin{pmatrix} -\frac{\partial_z}{i} + \mu - E & p_- \\ p_+ & \frac{\partial_z}{i} + \mu - E \end{pmatrix} f_R \pm m f_L = 0 \quad (\text{C5b})$$

$$\begin{pmatrix} -\frac{\partial_z}{i} - \mu - E & -p_- \\ -p_+ & \frac{\partial_z}{i} - \mu - E \end{pmatrix} f_L + m f_R = 0 \quad (\text{C5c})$$

$$\begin{pmatrix} \frac{\partial_z}{i} + \mu - E & -p_- \\ -p_+ & -\frac{\partial_z}{i} + \mu - E \end{pmatrix} f_L \pm m f_R = 0 \quad (\text{C5d})$$

with $p_{\pm} \equiv p_x \pm ip_y$.

1. Even parity pairing

When the pairing gap is parity even (upper sign), we can find the following four zero energy solutions at $m = p_x = p_y = 0$:

$$\begin{pmatrix} f_R \\ f_L \end{pmatrix} \propto \begin{pmatrix} e^{i\mu z} \\ 0 \\ 0 \\ 0 \end{pmatrix}, \quad \begin{pmatrix} 0 \\ e^{-i\mu z} \\ 0 \\ 0 \end{pmatrix}, \quad \begin{pmatrix} 0 \\ 0 \\ e^{-i\mu z} \\ 0 \end{pmatrix}, \quad \begin{pmatrix} 0 \\ 0 \\ 0 \\ e^{i\mu z} \end{pmatrix}. \quad (\text{C6})$$

By evaluating matrix elements of the perturbation Hamiltonian

$$\delta \mathcal{H} = \begin{pmatrix} \alpha_x p_x + \alpha_y p_y + \beta m & 0 \\ 0 & -\alpha_x p_x - \alpha_y p_y - \beta m \end{pmatrix} \quad (\text{C7})$$

with respect to the corresponding four zero energy eigenfunctions $\phi_{0,0}(z)$ in Eq. (C3), we obtain the following effective 2D Hamiltonian:

$$\mathcal{H}_{2D} = \begin{pmatrix} 0 & v^* p_- & v^* m & 0 \\ v p_+ & 0 & 0 & v m \\ v m & 0 & 0 & -v p_- \\ 0 & v^* m & -v^* p_+ & 0 \end{pmatrix} \quad (\text{C8})$$

with the velocity v defined in Eq. (54). Its energy eigenvalues are given by $E = \pm |v| \sqrt{m^2 + p_x^2 + p_y^2}$. This spectrum with $v = 1$ becomes exact for arbitrary p_x , p_y , and m in the special case where $\mu = 0$.

2. Odd parity pairing

When the pairing gap is parity odd (lower sign), we can find the following four zero energy solutions at $p_x = p_y = 0$:

$$\begin{aligned}
\begin{pmatrix} f_R \\ f_L \end{pmatrix} &\propto \begin{pmatrix} \mu + \sqrt{\mu^2 - m^2} \\ 0 \\ m \\ 0 \end{pmatrix} e^{i\sqrt{\mu^2 - m^2}z}, \\
\begin{pmatrix} 0 \\ \mu + \sqrt{\mu^2 - m^2} \\ 0 \\ m \end{pmatrix} &e^{-i\sqrt{\mu^2 - m^2}z}, \\
\begin{pmatrix} m \\ 0 \\ \mu + \sqrt{\mu^2 - m^2} \\ 0 \end{pmatrix} &e^{-i\sqrt{\mu^2 - m^2}z}, \\
\begin{pmatrix} 0 \\ m \\ 0 \\ \mu + \sqrt{\mu^2 - m^2} \end{pmatrix} &e^{i\sqrt{\mu^2 - m^2}z}.
\end{aligned} \tag{C9}$$

Note that the corresponding four zero energy eigenfunctions $\phi_{0,0}(z)$ in Eq. (C3) are normalizable in the z direction as long as $m^2 < \mu^2 + \Delta_\infty^2$. By evaluating matrix elements of the perturbation Hamiltonian

$$\delta\mathcal{H} = \begin{pmatrix} \alpha_x p_x + \alpha_y p_y & 0 \\ 0 & -\alpha_x p_x - \alpha_y p_y \end{pmatrix} \tag{C10}$$

with respect to the four zero energy eigenfunctions, we obtain the following effective 2D Hamiltonian:

$$\mathcal{H}_{2D} = \begin{pmatrix} 0 & v^* p_- & 0 & 0 \\ v p_+ & 0 & 0 & 0 \\ 0 & 0 & 0 & -v p_- \\ 0 & 0 & -v^* p_+ & 0 \end{pmatrix} \tag{C11}$$

for $m^2 < \mu^2$ with the velocity v defined in Eq. (58) and

$$\mathcal{H}_{2D} = \begin{pmatrix} 0 & 0 & 0 & -iv p_- \\ 0 & 0 & -iv p_+ & 0 \\ 0 & iv p_- & 0 & 0 \\ iv p_+ & 0 & 0 & 0 \end{pmatrix} \tag{C12}$$

for $\mu^2 < m^2 < \mu^2 + \Delta_\infty^2$ with the velocity v defined in Eq. (59). Their energy eigenvalues are given by $E = \pm |v| \sqrt{p_x^2 + p_y^2}$. This spectrum with $v = 1$ becomes exact for arbitrary p_x and p_y in the special case where $\mu = 0$.

-
- [1] D.J. Thouless, M. Kohmoto, M.P. Nightingale, and M. den Nijs, Phys. Rev. Lett. **49**, 405 (1982).
[2] M. Kohmoto, Ann. Phys. (N.Y.) **160**, 343 (1985).
[3] Q. Niu, D.J. Thouless, and Y.-S. Wu, Phys. Rev. B **31**, 3372 (1985).
[4] C.L. Kane and E.J. Mele, Phys. Rev. Lett. **95**, 226801 (2005).
[5] B.A. Bernevig and S.-C. Zhang, Phys. Rev. Lett. **96**, 106802 (2006).
[6] B.A. Bernevig, T.L. Hughes, and S.-C. Zhang, Science **314**, 1757 (2006).
[7] M. König *et al.*, Science **318**, 766 (2007).
[8] L. Fu, C.L. Kane, and E.J. Mele, Phys. Rev. Lett. **98**, 106803 (2007).
[9] J.E. Moore and L. Balents, Phys. Rev. B **75**, 121306 (2007).
[10] R. Roy, Phys. Rev. B **79**, 195322 (2009).
[11] D. Hsieh *et al.*, Nature (London) **452**, 970 (2008).
[12] D. Hsieh *et al.*, Science **323**, 919 (2009); Nature (London) **460**, 1101 (2009).
[13] Y. Xia *et al.*, Nature Phys. **5**, 398 (2009).
[14] H. Zhang *et al.*, Nature Phys. **5**, 438 (2009).
[15] Y.L. Chen *et al.*, Science **325**, 178 (2009).
[16] N. Read and D. Green, Phys. Rev. B **61**, 10267 (2000).
[17] Y. Maeno *et al.*, Nature (London) **372**, 532 (1994).
[18] R. Jackiw and P. Rossi, Nucl. Phys. **B190**, 681 (1981).
[19] L. Fu and C.L. Kane, Phys. Rev. Lett. **100**, 096407 (2008).
[20] A.P. Schnyder, S. Ryu, A. Furusaki, and A. W. W. Ludwig, Phys. Rev. B **78**, 195125 (2008).
[21] R. Roy, arXiv:0803.2868.
[22] X.-L. Qi, T.L. Hughes, S. Raghu, and S.-C. Zhang, Phys. Rev. Lett. **102**, 187001 (2009).
[23] See also, G.E. Volovik, *The Universe in a Helium Droplet* (Clarendon Press, Oxford, 2003).
[24] For a recent review, see M.G. Alford, A. Schmitt, K. Rajagopal, and T. Schafer, Rev. Mod. Phys. **80**, 1455 (2008).
[25] M.R. Zirnbauer, J. Math. Phys. (N.Y.) **37**, 4986 (1996).
[26] A. Altland and M.R. Zirnbauer, Phys. Rev. B **55**, 1142 (1997).
[27] X.-L. Qi, T.L. Hughes, and S.-C. Zhang, arXiv:0908.3550.
[28] V. Gurarie and L. Radzihovsky, Phys. Rev. B **75**, 212509 (2007); see also Sec. VIII in Ann. Phys. (N.Y.) **322**, 2 (2007).
[29] M.G. Alford, K. Rajagopal, and F. Wilczek, Phys. Lett. B **422**, 247 (1998).
[30] R. Rapp, T. Schafer, E.V. Shuryak, and M. Velkovsky, Phys. Rev. Lett. **81**, 53 (1998).
[31] E.J. Weinberg, Phys. Rev. D **24**, 2669 (1981).
[32] C. Caroli, P.G. de Gennes, and J. Matricon, Phys. Lett. **9**, 307 (1964).
[33] G.E. Volovik, Lect. Notes Phys. **718**, 31 (2007).
[34] M.M. Forbes and A.R. Zhitnitsky, Phys. Rev. D **65**, 085009 (2002).
[35] K. Iida and G. Baym, Phys. Rev. D **66**, 014015 (2002).
[36] D.T. Son and M.A. Stephanov, Phys. Rev. D **61**, 074012 (2000); **62**, 059902 (2000).
[37] S. Yasui, K. Itakura, and M. Nitta, arXiv:1001.3730.